

shown the thermal treatment in condition of low air humidity under reduced pressure leads to the total diminishing to  $V^{IV}$  species.

The quantum yield of conversion of absorbed photons to electrical current was determined to be about 2%, assuming that all incident photons have the same 435 nm wavelength. This quantum yield is not large, but could be increased. For example, the excited state (eq 1) likely is quenched immediately after its creation, probably by water molecules present in the gel structure and thus photocurrent is diminished. The vanadium pentoxide conductivity influences the transport of an electron to the

electrode or holes to the solution and is affected by water concentration and  $V^{(IV)}$  concentration in the gel. A better understanding of the role of  $H_2O$  and  $V^{IV}$  in gel structure, charge transfer and their relation may enable an increase in photocurrent by systematic variation of the water and  $V^{IV}$  concentration. Thus, the gel current can be optimized.

**Acknowledgment.** Supported by the Army Research Office (RTP, North Carolina).

**Registry No.** PC, 108-32-7;  $In_2O_3$ , 1312-43-2;  $VO(OCH_2CH_3)_3$ , 1686-22-2;  $V_2O_5$ , 1314-62-1;  $H_2SO_4$ , 7664-93-9; ammonium metavanadate, 7803-55-6.

## Discrete Layers of Ordered $C_{60}$ Molecules in the Cocrystal $C_{60} \cdot CH_2I_2 \cdot C_6H_6$ : Synthesis, Crystal Structure, and $^{13}C$ NMR Properties

Urs Geiser,\* S. Kalyan Kumar, Bradley M. Savall, Scott S. Harried, K. Douglas Carlson,\* Paul R. Mobley, H. Hau Wang,\* Jack M. Williams,\* and Robert E. Botto\*

Chemistry and Materials Science Divisions, Argonne National Laboratory, 9700 S. Cass Avenue, Argonne, Illinois 60439

W. Liang and M.-H. Whangbo\*

Department of Chemistry, North Carolina State University, Raleigh, North Carolina 27695

Received May 26, 1992. Revised Manuscript Received July 24, 1992

The first crystals containing crystallographically ordered (at room temperature) unmodified fullerene ( $C_{60}$ ) molecules, with chemical composition  $C_{60} \cdot CH_2I_2 \cdot C_6H_6$ , have been prepared. The fullerene molecules are arranged in novel hexagonally close-packed layers, separated by the solvent components. A monoclinic (space group  $C2/c$ ) crystal structure of  $C_{60} \cdot CH_2I_2 \cdot C_6H_6$  was determined at room temperature [lattice parameters:  $a = 21.239$  (7) Å,  $b = 17.403$  (4) Å,  $c = 10.106$  (2) Å,  $\beta = 106.03$  (2)°,  $V = 3590$  (2) Å<sup>3</sup>] and at 122 K [ $a = 21.024$  (7) Å,  $b = 17.298$  (4) Å,  $c = 10.043$  (2) Å,  $\beta = 105.93$  (2)°,  $V = 3512$  (2) Å<sup>3</sup>]. The ordered nature (on the X-ray time scale) of the compound allows a detailed determination and discussion of the intermolecular interactions between neighboring fullerene molecules as well as between the  $C_{60}$  and the solvent molecules. Solid-state  $^{13}C$  NMR under MAS shows three distinct resonances for  $C_{60}$ , benzene and  $CH_2I_2$ ; static NMR measurements set a lower limit for the rate of molecular rotation of  $C_{60}$  on a time scale of tens of microseconds.

### Introduction

When macroscopic quantities of buckminsterfullerene,  $C_{60}$ , became available,<sup>1</sup> attempts were immediately made to confirm the proposed truncated-icosahedral geometry of the molecule by use of diffraction techniques. Shortly thereafter it was demonstrated that crystals of pure  $C_{60}$  consisted of closely packed spherical carbon molecules in a face-centered cubic array (space group  $Fm\bar{3}m$ ), but the molecules were completely disordered crystallographically, undergoing essentially free rotation at a rate of more than a billion times per second.<sup>2,3</sup> Thus, neither atomic coordinates nor detailed investigation of the  $C_{60}$ - $C_{60}$  interactions could be obtained from diffraction experiments at room temperature. The geometry of the molecule was subsequently demonstrated at atomic resolution in the crystal structures of the ordered derivatives  $C_{60}[OsO_4(4\text{-tert-butylpyridine})_2]$ <sup>4</sup> and  $[(C_6H_5)_3P]_2Pt(\eta^2-C_{60}) \cdot C_4H_8O$ ,<sup>5</sup> where the bulky "tagging" substituents prevented the

otherwise free rotation of the fullerene molecule. Upon cooling, solid  $C_{60}$  undergoes a phase transition at 249 K to a primitive crystal lattice space group  $Pa\bar{3}$ . The symmetry-lowering nature of the phase transition normally results in twinned crystals when they are cooled through the phase transition. The structure of the low-temperature phase was investigated at 110 K on a twinned crystal<sup>6</sup> and at 5 K by use of powder neutron diffraction.<sup>7</sup> Both low-

(1) Krätschmer, W.; Lamb, L. D.; Fostiropoulos, K.; Huffman, D. R. *Nature* 1990, 347, 354.

(2) Yannoni, C. S.; Johnson, R. D.; Meijer, G.; Bethune, D. S.; Salem, J. R. *J. Phys. Chem.* 1991, 95, 9.

(3) Tycko, R.; Haddon, R. C.; Dabbagh, G.; Glarum, S. H.; Douglass, D. C.; Mujsce, A. M. *J. Phys. Chem.* 1991, 95, 518.

(4) Hawkins, J. M.; Meyer, A.; Lewis, T. A.; Loren, S.; Hollander, F. *J. Science* 1991, 252, 312.

(5) Fagan, P. J.; Calabrese, J. C.; Malone, B. *Science* 1991, 252, 1160.

(6) Liu, S.; Lu, Y.-J.; Kappes, M. M.; Ibers, J. A. *Science* 1991, 254, 408.

(7) David, W. I. F.; Ibberson, R. M.; Matthewman, J. C.; Prassides, K.; Dennis, T. J. S.; Kroto, H. W.; Taylor, R.; Walton, D. R. M. *Nature* 1991, 353, 147.

\* To whom correspondence may be addressed.

**Table I. Crystallographic Data, Data Collection Parameters, and Structure Refinement for  $C_{60} \cdot CH_2I_2 \cdot C_6H_6$** 

	$T = 295\text{ K}$	$T = 122\text{ K}$
$a$ (Å)	21.239 (7)	21.024 (7)
$b$ (Å)	17.403 (4)	17.298 (4)
$c$ (Å)	10.106 (2)	10.043 (2)
$\beta$ (deg)	106.03 (2)	105.93 (2)
$V$ (Å <sup>3</sup> )	3590 (2)	3512 (2)
$Z$	4	4
space group	$C2/c$	$C2/c$
scan type	$\theta/2\theta$ , 2.1–2.5°, 1.5° min <sup>-1</sup>	$\theta/2\theta$ , 2.1–2.5°, 1.5–3° min <sup>-1</sup>
angle range	$4^\circ \leq 2\theta \leq 48^\circ$	$4^\circ \leq 2\theta \leq 55^\circ$
no. of reflns measd	3262	4642
no. of unique reflns	2823	4040
no. of obsd reflns	2144 ( $F > 3\sigma$ )	3276 ( $F > 4\sigma$ )
abs coeff (cm <sup>-1</sup> )	17.9	17.9
cryst size (mm <sup>3</sup> )	$0.02 \times 0.2 \times 0.2$	$0.04 \times 0.2 \times 0.2$
transmission factors	0.77–0.95	0.64–0.94
no. of variables	163	301
$R$	0.133	0.063
$R_w$	0.107	0.05
goodness of fit	3.48	2.34

temperature structures show ordered  $C_{60}$  molecules with average C–C distances of 1.35–1.40 Å for the bonds joining two six-membered rings and 1.38–1.56 Å for those joining five- and six-membered rings. This observation of disordered molecules at high temperature and twinned crystals at low-temperature calls for the investigation of new systems in which these difficulties are absent if an understanding of intermolecular  $C_{60}$  interactions are to be elucidated. In this paper, we demonstrate that cocrystallization of  $C_{60}$  with the appropriate solvent mixture (as suggested by Liu et al.<sup>6</sup>) leads to a structure of lower symmetry in which the fullerene molecules are indeed crystallographically ordered, even at room temperature.

### Experimental Section

Crystals of  $C_{60} \cdot CH_2I_2 \cdot C_6H_6$  were grown by slow evaporation of ca. 20 mL of a saturated solution of  $C_{60}$  (generated and purified by the method described earlier<sup>8</sup>) in benzene, either with an excess (typically, 10-fold) of  $CH_2I_2$  at room temperature or from a 1:1  $C_{60} \cdot CH_2I_2$  mixture after reflux in ca. 20 mL of benzene for 24 h. The crystals formed were collected by Büchner filtration and dried in air. They were typically dark brown to black, thin elongated-hexagonal plates, stable in air. In contrast, a 1:1  $C_{60} \cdot CH_2I_2$  mixture left at room temperature gave only chunky crystals (presumably  $C_{60}$  or a solvate of  $C_{60}$  with only benzene) which showed no recognizable X-ray diffraction pattern. However, the plate-like single crystals of  $C_{60} \cdot CH_2I_2 \cdot C_6H_6$  exhibited a sharp diffraction pattern suitable for crystallographic analysis (for details, see Table I), which also established the composition of the material. The iodine atom position was located by the use of the Patterson method, and the structure completed by several cycles of electron density maps (later, difference Fourier maps) and structure factor calculations.<sup>9</sup> The low-temperature data set was collected with a slightly larger crystal. The temperature of  $122 \pm 2\text{ K}$  was obtained by use of a nitrogen flow cooling device.

Solid-state <sup>13</sup>C NMR spectra were recorded at 2.3 and 7.05 T (25.18 and 75.47 MHz for <sup>13</sup>C, respectively) on Bruker Instruments spectrometers, Models CXP-100 and AM-300, in the pulse Fourier transform mode with quadrature phase detection. The Bruker AM-300 spectrometer was fitted with a solids NMR probe from Doty Scientific Instruments. The samples were placed in ceramic rotors; magic-angle spinning (MAS) experiments on the Bruker CXP-100 were carried out at approximately 4 kHz. Operating

parameters in ring-down elimination (RIDE) experiments<sup>10</sup> employed spectral widths of 10–20 kHz, 90° and 180° carbon pulse widths of 4.25 and 8.50 μs, an acquisition time of 50 ms, and a proton-decoupling field of 60 kHz. Static <sup>13</sup>C spectra were obtained using a recycle delay of 100 s. MAS spectra were acquired using a recycle delay of 1 s; between 40 and 60 K transients were collected for a typical spectrum. Linewidths of static spectra were evaluated using the line simulation routine provided with the Bruker software.

### Results and Discussion

The crystal structure determination of  $C_{60} \cdot CH_2I_2 \cdot C_6H_6$  carried out at room temperature showed that all buckminsterfullerene carbon atoms readily appeared as distinct peaks on the electron density maps, indicating a high degree of order. In addition to  $C_{60}$  and the methylene iodide molecule, a molecule of benzene was located. Refinement with isotropic thermal parameters for the 30 independent fullerene carbon atoms, anisotropic thermal parameters for the solvent atoms, and fixed hydrogen atom positions (163 variables, including one scale factor) converged to  $R = 0.133$ ,  $R_w = 0.107$ . An attempt to refine anisotropic thermal parameters for all carbon atoms was abandoned, partly because the number of variables exceeded one-seventh of the number of observed data, but primarily because some of the atoms refined with nonpositive definite thermal parameters, leading to instability in the refinement. An examination of those anisotropic thermal parameters which refined positive-definite showed that the thermal motion is almost entirely along the surface of the sphere of the molecule. This finding is corroborated by high correlations between the thermal parameters and the atom coordinates parallel to the molecule's surface. The nonpositiveness of the temperature factors indicates the failure of the harmonic approximation model. However, due to the limited number of observed data, no attempt was made to refine a model involving higher order tensors. The correlations between the positional and thermal parameters along the surface of the molecular sphere are undoubtedly responsible for the large variations among the observed bond lengths (1.1–1.8 Å).

Because of the thermal motion problems, we collected a second data set, with a slightly larger crystal, at  $122 \pm 2\text{ K}$  (nitrogen flow cooling device). No evidence of a phase transition was observed, and the lattice remained  $C$  centered (see Table I). The room-temperature refinement coordinates were used as starting parameters with hydrogen atoms included at fixed positions and isotropic temperature factors ( $B = 4.0$ ). All non-hydrogen atoms were refined with anisotropic thermal parameters. However, this refinement again led to non-positive-definite temperature factors on nine  $C_{60}$  carbon atoms. These atoms were then refined with a damping factor (applied shifts = 20% of calculated shifts to the thermal parameters on each cycle), starting from the isotropic values. The refinement improved, and the thermal parameters of only two atoms (C10 and C12) became non-positive-definite before the remaining variables converged satisfactorily. Thus, the thermal parameters of C10 and C12 were fixed at their values from the previous refinement cycle, and the remaining 301 parameters were refined one more time, leading to agreement factors  $R = 0.063$ ,  $R_w = 0.055$ , goodness-of-fit = 2.34. The largest calculated shift was  $1.8\sigma$  for  $\beta_{33}(C26)$ , and except for the atoms with problematic

(8) Wang, H. H.; Kini, A. M.; Savall, B. M.; Carlson, K. D.; Williams, J. M.; Lykke, K. R.; Wurz, P.; Parker, D. H.; Pellin, M. J.; Gruen, D. M.; Welp, U.; Kwok, W.-K.; Fleshler, S.; Crabtree, G. W. *Inorg. Chem.* 1991, 30, 2838.

(9) Strouse, C. *UCLA Crystallographic Package*; University of California, Los Angeles, 1985.

(10) Belton, P. S.; Cox, I. J.; Harris, R. K. *J. Chem. Soc., Faraday Trans. 2* 1985, 81, 63–75.

(11) Zhu, Q.; Cox, D. E.; Fischer, J. E.; Kniaz, K.; McGhie, A. R.; Zhou, O. *Nature* 1992, 355, 712.

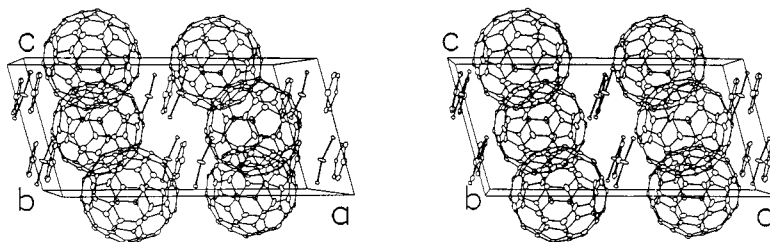


Figure 1. Stereoview of the unit cell of C<sub>60</sub>·CH<sub>2</sub>I<sub>2</sub>·C<sub>6</sub>H<sub>6</sub> approximately along the *b* axis. The novel fullerene layers (two per unit cell) are seen in an edge-on view.

Table II. Bond Distances (Averaged over Chemically Equivalent Bonds) in Several C<sub>60</sub> Structure Determinations<sup>a</sup>

compound	method	temp (K)	sym	<i>d</i> <sub>66</sub> (Å)	<i>d</i> <sub>56</sub> (Å)	ref
C <sub>60</sub>	NMR	77	<i>m</i> 5̄ <i>m</i>	1.400 (15)	1.450 (15)	16
C <sub>60</sub>	gas-phase electron diffraction	730	<i>m</i> 5̄ <i>m</i>	1.401 (10)	1.458 (6)	17
C <sub>60</sub>	twinned crystal, X-ray diffraction	110	3̄	1.355 (9)	1.467 (21)	6
C <sub>60</sub>	powder, neutron diffraction	5	3̄	1.34–1.39	1.38–1.56	7
C <sub>60</sub> (OsO <sub>4</sub> )(bp) <sub>2</sub> <sup>b</sup>	single crystal, X-ray diffraction	298?	1	1.391 (18)	1.455 (20)	7
[φ <sub>3</sub> P] <sub>2</sub> Pt(C <sub>60</sub> )·THF	single crystal, X-ray diffraction	203	1	1.366–1.412	1.420–1.487	4
C <sub>60</sub> ·CH <sub>2</sub> I <sub>2</sub> ·C <sub>6</sub> H <sub>6</sub>	single crystal, X-ray diffraction	122	1̄	1.388 (9) <sup>c</sup>	1.432 (5) <sup>c</sup>	5
				1.36 (5)	1.46 (6)	this work
				1.257–1.427	1.365–1.623	

<sup>a</sup> *d*<sub>66</sub> denotes a bond linking a five- and a six-membered ring, whereas *d*<sub>56</sub> indicates one joining two six-membered rings. In site symmetry *m*5̄*m* all bonds of a given type are equivalent, and the error shown indicates the estimated standard deviation given in the original literature. In lower symmetry cases, the rms deviation of the last digits is indicated, as well as a range of distances if available. <sup>b</sup>bp = 4-*tert*-butylpyridine. <sup>c</sup>The small "errors" given in ref 4 suggests that the values are standard errors of the mean,  $\sigma(\bar{x})$ , rather than the rms deviations,  $\bar{\sigma}(x)$ , are quoted.  $\sigma(\bar{x}) = (\bar{\sigma}^2(x)/n)^{1/2}$  (where *n* is the number of contributing terms).

thermal parameters, all other shifts were smaller than 0.05σ. Several diffuse maxima of residual electron density (ca. 1 e/Å<sup>3</sup>) on the surface of the C<sub>60</sub> molecule were observed in a final difference map.

The crystal structure of C<sub>60</sub>·CH<sub>2</sub>I<sub>2</sub>·C<sub>6</sub>H<sub>6</sub> contains novel close-packed layers of C<sub>60</sub> parallel to the *bc* plane (corresponding to the plate direction of the crystal morphology); see Figure 1. Each fullerene molecule is located on a center of inversion, and the two inequivalent fullerene center-to-center distances (at 295 K) of 10.106 and 10.062 Å, respectively, are essentially those found in cubic C<sub>60</sub> (*a*<sub>0</sub>/√2 = 10.04 Å, with *a*<sub>0</sub> = 14.2 Å). These layers are spaced ca. 2.0 Å further apart than in the fcc lattice of pure C<sub>60</sub>, thereby accommodating the methylene iodide and benzene molecules which are both situated on two-fold rotation axes. Only one other layered C<sub>60</sub> compound is known to date, i.e., C<sub>60</sub>I<sub>4</sub>.<sup>11</sup> However, in the latter both C<sub>60</sub> and the iodine molecules are heavily disordered, based on powder diffraction data.

An ideal truncated icosahedron consists of 12 regular pentagons and 20 regular hexagons. There are two kinds of edges (C–C bonds), 20 of those joining two hexagons (*d*<sub>66</sub>) and 40 of those joining a pentagon with a hexagon (*d*<sub>56</sub>). In this determination, one-half of the fullerene molecule consisted of crystallographically nonequivalent atoms, and thus 10 of the 66-bond lengths and 20 of the 56-bond lengths are independently determined with an estimated standard deviation of ca. 0.01 Å for the 122 K structure. A range of bond lengths is observed for each type of bond (Table II), but the average values agree very well with the published numbers from other determinations.<sup>4–7</sup> It is possible that the differences among chemically equivalent bond lengths are due to the variation in the nonbonded environment, but it is more likely that the variations are an artifact of the thermal motion model. The bonds on the fringe of the ranges for the two chemical types do involve atoms that presented difficulties in the refinement of the thermal parameters.

Ideal pentagons and hexagons have bond angles of 108° and 120°, respectively. The observed range of the former

is 102.5–111.6° and of the latter 115.9–126.0°, with individual esd's of 0.6–1.0°. The average values are 108.00° and 119.99°, indicating that the polyhedral faces are virtually planar. The bond lengths and angles of the CH<sub>2</sub>I<sub>2</sub> and C<sub>6</sub>H<sub>6</sub> moieties are in their expected ranges: *d*<sub>C–I</sub> = 2.126 (7) Å, ∠<sub>I–C–I</sub> = 114.3 (6)° for the methylene iodide molecule; *d*<sub>C–C</sub> = 1.37 (1)–1.41 (1) Å, ∠<sub>C–C–C</sub> = 117.5 (8)–122.2 (8)° for the benzene molecule.

This structure determination presents a unique opportunity to study the intermolecular interactions within the unusual C<sub>60</sub> sheets and to compare them with those found in the three-dimensional structure of pure C<sub>60</sub>, as well as with theoretical predictions. Due to the symmetry of the layers, two distinct interaction motifs are found. Motif 1, shown in Figure 2a, occurs at four of the nearest-neighbor contacts between adjacent C<sub>60</sub> molecules. The molecules involved are related by a screw rotation (simultaneously by a glide reflection because of the inversion center found at the center of the fullerene molecule). This contact is formed by the skewed overlap of two 56-bonds (C6–C10 and C24–C25, respectively), leading to the three short contacts indicated in Figure 2a. For comparison, the van der Waals diameter of a carbon atom is ca. 3.40 Å.<sup>12</sup> The other contact, motif 2 (shown in Figure 2b), involves C<sub>60</sub> molecules related by a unit cell translation along the *c* axis, thus also by a center of inversion located between the molecules. This contact is formed by the slipped overlap of two hexagons, leading to the shortest C4...C12 interactions indicated in Figure 2b. These contacts are slightly longer than the sum of the van der Waals radii (3.40 Å). In pure C<sub>60</sub> at 5 K a different packing motif was found.<sup>7</sup> The intermolecular contacts consisted of a 66-bond on top of a pentagon, and the shortest C...C distances were 3.12 and 3.27 Å.

Various theoretical papers have dealt with the energetics of interacting C<sub>60</sub> molecules. Guo et al.<sup>13</sup> concluded that the most favorable interaction was via facing hexagons,

(12) Bondi, A. *J. Phys. Chem.* 1964, 68, 441.

(13) Guo, Y.; Karasawa, N.; Goddard III, W. A. *Nature* 1991, 351, 464.

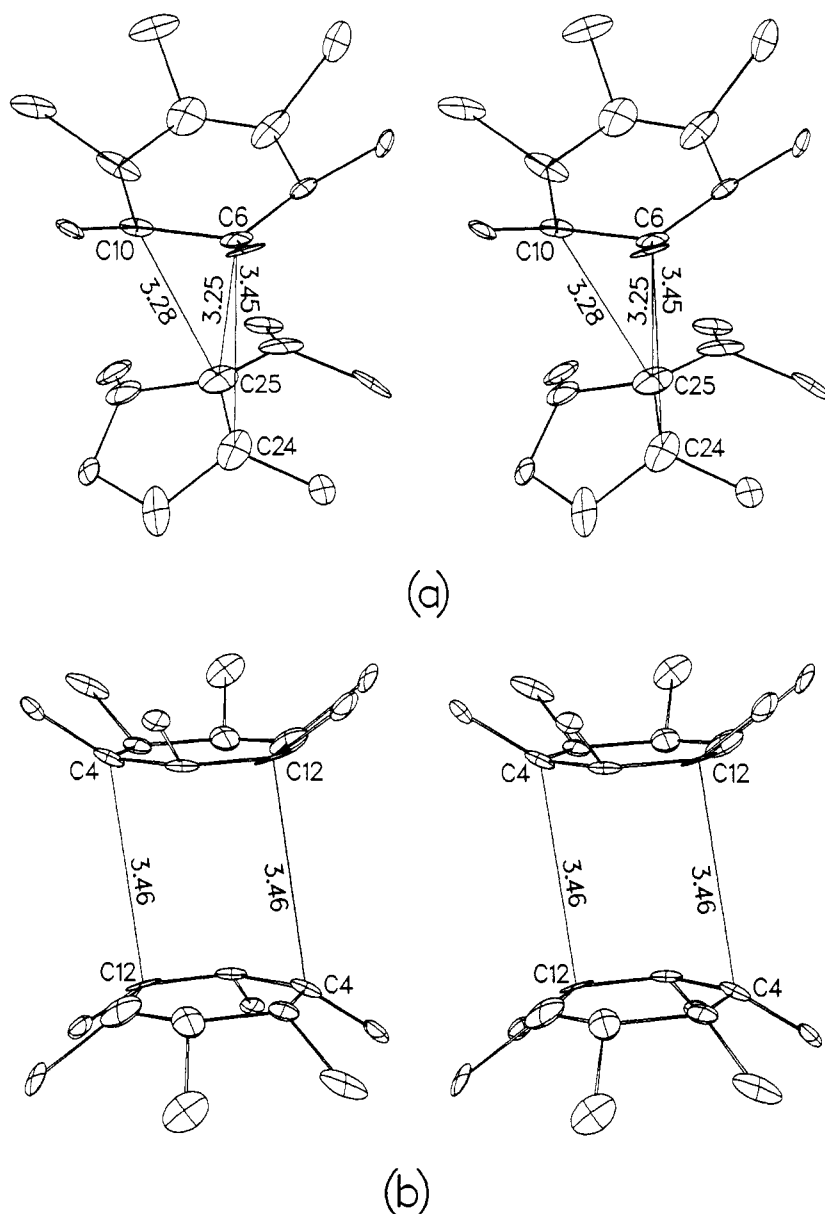


**Figure 2.** Stereoviews of the intermolecular  $C_{60}\cdots C_{60}$  interactions. (a) Interaction between molecules related by screw rotation/glide reflection (motif 1). (b) Interaction between translationally related molecules (motif 2). In both figures the shortest  $C\cdots C$  contacts are drawn with thin lines, and their lengths (angstroms) are indicated in the figure.

whereas Gunnarson et al.<sup>14</sup> decided that facing 56-bonds would lead to a lower energy. The data on pure  $C_{60}$  are more consistent with the second assumption, and our observation that the shorter contacts are found in packing motif 1 (vide supra, skewed 56-bonds), also supports Gunnarson's<sup>14</sup> conclusion. However, the most electrostatically attractive intermolecular contact in  $C_{60}\cdot CH_2I_2\cdot C_6H_6$  is expected to be the  $I\cdots C$  interaction because of the dipolar nature of the methylene C-I bond. The iodine atom (by symmetry, both iodine atoms of the  $CH_2I_2$  molecule are involved in equivalent interactions with fullerene molecules located on different layers) is located approximately over a 56-bond C2-C3 (see Figure 3a), and the  $I\cdots C$  distances (3.29 and 3.54 Å) are considerably shorter than the sum of the van der Waals radii of 3.68 Å.<sup>12</sup> In contrast, in complexes of aromatic hydrocarbons with molecular halogens or halocarbons, e.g., *p*-xylene- $CBr_4$ ,<sup>15</sup> the halogen atom is located over the center of a

ring, and at a distance approximately equal to the sum of the van der Waals radii. Due to the high ionization potential of  $CH_2I_2$  any charge transfer between the fullerene molecule and the iodine atom is unlikely to be extensive. The crystals of  $C_{60}\cdot CH_2I_2\cdot C_6H_6$  are electrically insulating (four-probe resistivity measurement) and show no ESR signal at room temperature, thus indicating no significant charge transfer. Similarly, the infrared spectrum is a superposition (shifts  $<3\text{ cm}^{-1}$ ) of the spectra of the individual components,  $C_{60}$ ,  $CH_2I_2$ , and benzene.

The benzene molecule is wedged between two fullerene molecules (located on different layers), to form some short  $C\cdots C$  intermolecular contacts; see Figure 3b. The  $C\cdots C$  distances of 3.16 (1) and 3.28 (1) Å are again substantially smaller than the van der Waals radii sum of 3.4 Å. Each  $C_{60}$  molecule is in close contact with six other fullerene

(15) Strieter, F. J.; Templeton, D. H. *J. Chem. Phys.* **1962**, *37*, 161.

(16) Yannoni, C. S.; Bernier, P. P.; Bethune, D. S.; Meijer, G.; Salem, J. R. *J. Am. Chem. Soc.* **1991**, *113*, 3190.

(17) Hedberg, K.; Hedberg, L.; Bethune, D. S.; Brown, C. A.; Dorn, H. C.; Johnson, R. D.; de Vries, M. *Science* **1991**, *254*, 410.

(14) Gunnarson, O.; Satpathy, S.; Jepsen, O.; Andersen, O. K. *Phys. Rev. Lett.* **1991**, *67*, 3002.

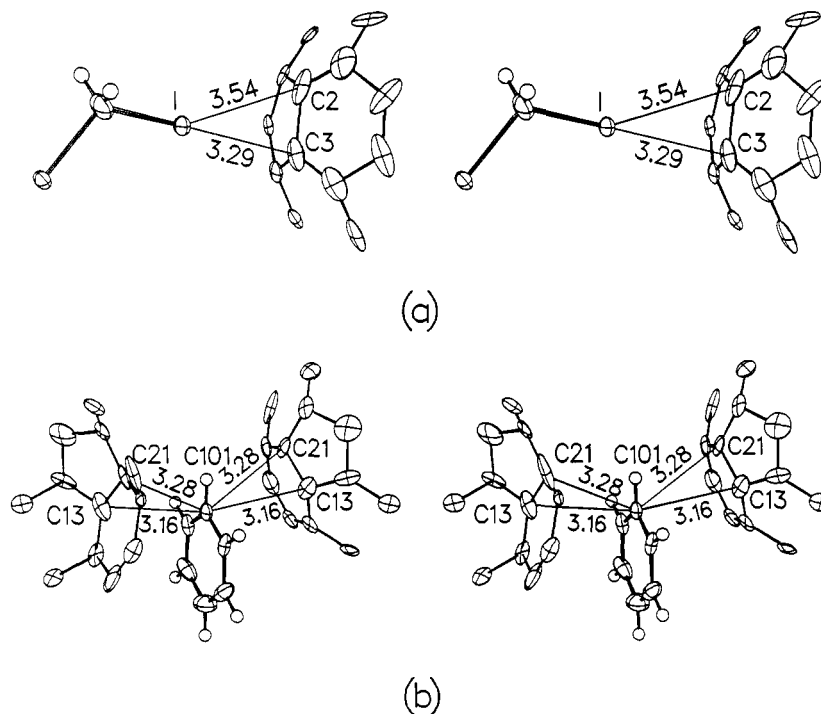


**Figure 3.** Stereoview of the solvent... $C_{60}$  interactions (a,  $CH_2I_2$ ; b,  $C_6H_6$ ) in  $C_{60}\cdot CH_2I_2\cdot C_6H_6$ . The short intermolecular contacts are indicated with thin lines, and their lengths given in angstroms.

molecules within the layer, two near iodine atoms on opposite sides of the layer, and two benzene carbon atoms, also on opposite sides (acting almost clamplike). All of these short intermolecular contacts exert sufficient electrostatic forces on the  $C_{60}$  molecules to halt (on the X-ray time scale) the free rotation of the latter even at room temperature.

Solid-state 25-MHz  $^{13}C$  NMR spectra of  $C_{60}\cdot CH_2I_2\cdot C_6H_6$  are shown in Figure 4. The MAS spectrum (a) exhibits two sharp resonance lines at 146.7 and 133.1 ppm and a somewhat broad resonance at approximately 35 ppm, corresponding to carbon atoms of  $C_{60}$ , benzene and methylene iodide, respectively. The recycle delay time was chosen to enhance the weak carbon signal of methylene iodide; hence integrated signal intensities in the spectrum do not accurately reflect the number of carbon atoms in each chemical environment. Broadening of the carbon resonance of methylene iodide results from residual quadrupole coupling to iodine due to restricted motion in the crystal lattice. The static spectrum (b) of the  $C_{60}$  cocrystal recorded at room temperature shows a single Gaussian line at 146.7 ppm with a fwhm = 147 Hz. The  $C_{60}$  resonance in the static spectrum recorded at a carbon frequency of 75 MHz has a fwhm = 240 Hz. The narrow line widths observed at both frequencies indicate that the  $C_{60}$  molecules in the cocrystal rotate rapidly and *nearly isotropically* relative to the NMR time scale defined by the inverse of the chemical shift anisotropies (CSA) of the aromatic carbons in  $C_{60}$ . The CSA powder pattern for solid  $C_{60}$  is approximately 200 ppm in width,<sup>2,3</sup> and thus the rotational correlation time of  $C_{60}$  in the co-crystal must be short compared to the inverse CSA width, or less than about 70  $\mu s$ .

### Conclusions

We have shown that  $C_6H_6$  and  $CH_2I_2$  cocrystallize with buckminsterfullerene to form *ordered layers* of  $C_{60}$  molecules. The contact distance between the solvent-iodine atom and the fullerene molecule is extremely short, 0.4 Å shorter than the sum of the van der Waals radii, but no

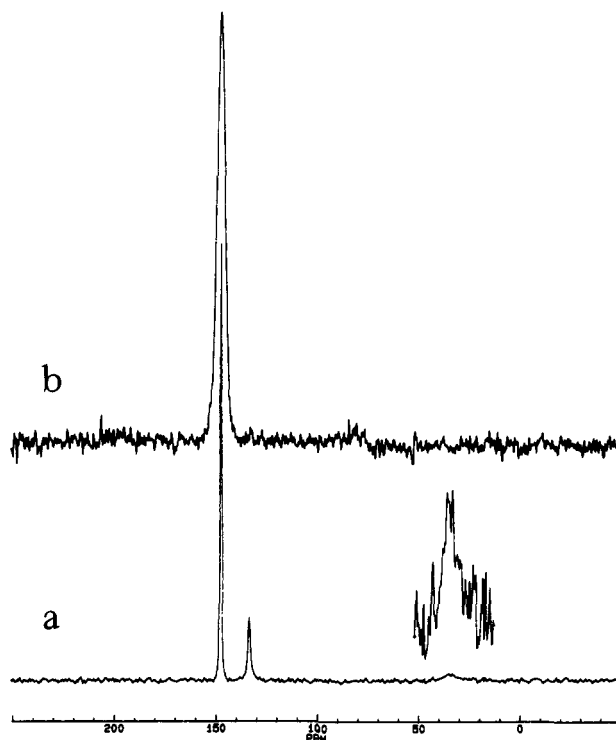


**Figure 4.** Solid-state MAS (a) and static (b)  $^{13}C$  NMR spectra of polycrystalline  $C_{60}\cdot CH_2I_2\cdot C_6H_6$ .

charge transfer is apparent. The  $C_{60}$  molecules interact among themselves more closely through overlapping 5b-bonds than through facing rings.

Even though the crystallographic analysis of  $C_{60}\cdot CH_2I_2\cdot C_6H_6$  shows the fullerene molecules to be ordered on the X-ray time scale, NMR experiments indicate dynamic effects. Static  $^{13}C$  spectra taken at two field strengths demonstrate that the rotational correlation time of  $C_{60}$  in the cocrystal is shorter than 70  $\mu s$ . This upper limit is at least 4 orders of magnitude larger than the lower limit, i.e., that of pure  $C_{60}$  (<1 ns).<sup>2</sup> The source of the Gaussian line

shape (rather than Lorentzian) for a freely rotating molecule is not fully understood at this moment. An attractive possibility which is consistent with the crystallographic observation of distinct electron density peaks (ordered atomic positions) would be a restricted (jumping) rotation of the molecule such that each atom spends a considerable amount at or near its equilibrium position ("ratchet motion"). A thorough investigation of the temperature dependence of the  $^{13}\text{C}$  NMR lineshape and spin-lattice relaxation time ( $T_1$ ) to probe the details of molecular motion in  $\text{C}_{60}\cdot\text{CH}_2\text{I}_2\cdot\text{C}_6\text{H}_6$  is planned.

The layered nature of the  $\text{C}_{60}\cdot\text{CH}_2\text{I}_2\cdot\text{C}_6\text{H}_6$  crystals opens the possibility, through replacement of some or all of the benzene or methylene iodide molecules with a suitable cation, to build salts of fulleride anions if charge transfer to the layers can be induced. Such salts should be good two-dimensional electrical conductors, possibly even superconductors.

**Acknowledgment.** Work at Argonne National Laboratory and North Carolina State University is sponsored by the U.S. Department of Energy, Office of Basic Energy Sciences, Divisions of Materials and Chemical Sciences,

under Contract W-31-109-ENG-38 and Grant DE-FG05-86ER45259, respectively. B.M.S., S.S.H., and P.R.M. are student undergraduate research participants, sponsored by the Argonne Division of Educational Programs, from the University of Wisconsin at Stevens Point, WI, and Platteville, WI, and from Willamette University, Salem, OR, respectively. We thank Drs. Aravinda M. Kini and Constantino S. Yannoni for fruitful discussions.

**Note added in proof:** A further analysis of the low-temperature X-ray diffraction data revealed the presence of a minor fraction (<30%) of the  $\text{C}_{60}$  molecules in a different orientation than that reported here. We thank Dr. Marilyn M. Olmstead and Mr. Bruce C. Noll, University of California at Davis, for suggesting the reanalysis.

**Registry No.**  $\text{C}_{60}\cdot\text{CH}_2\text{I}_2\cdot\text{C}_6\text{H}_6$ , 143124-00-9.

**Supplementary Material Available:** Atomic coordinates and thermal parameters for  $\text{C}_{60}\cdot\text{CH}_2\text{I}_2\cdot\text{C}_6\text{H}_6$  at 295 K and at 122 K (6 pages); observed and calculated structure factors (24 pages). Ordering information is given on any current masthead page.

## Scanning Tunneling Microscopy of the Organic Conductor $[(\eta\text{-C}_5\text{Me}_5)_2\text{Ru}(\eta^6, \eta^6\text{-}[2_2](1,4)\text{-cyclophane})][\text{TCNQ}]_4$

Shulong Li, Henry S. White, and Michael D. Ward\*

Department of Chemical Engineering and Materials Science, University of Minnesota,  
 Amundson Hall, 421 Washington Ave. SE, Minneapolis, Minnesota 55455

Received June 5, 1992

Scanning tunneling microscopy (STM) studies of the (001) and (010) faces, of the molecular semiconductor  $[(\eta\text{-C}_5\text{Me}_5)_2\text{Ru}(\eta^6, \eta^6\text{-}[2_2](1,4)\text{-cyclophane})]^{2+}[\text{TCNQ}]_4^{2-}$  (1, TCNQ = tetracyanoquinodimethane) are reported. The lattice constants determined from the density of states corrugation of the STM images are  $a = 13.8 \pm 0.3 \text{ \AA}$ ,  $b = 15.9 \pm 0.2 \text{ \AA}$ ,  $c = 16.6 \pm 2 \text{ \AA}$ ,  $\beta = 88^\circ \pm 2^\circ$ ,  $\gamma = 82^\circ \pm 2^\circ$ , in good agreement with the X-ray crystal structure. STM images of both faces reveal local density of states (LDOS) associated with stacking of TCNQ molecules along the [100] direction in two crystallographically unique stacks. The tunneling current contrast conforms to the tetrameric periodicity of the TCNQ stacks observed in the crystal structure. Columnar regions of negligible tunneling current on the *ac* face are attributed to stacks of  $(\eta\text{-C}_5\text{Me}_5)_2\text{Ru}(\eta^6, \eta^6\text{-}[2_2](1,4)\text{-cyclophane})^{2+}$  dications. Each TCNQ column exhibits a tunneling current corrugation repeating at intervals of  $a$  that is attributed to tunneling into the conduction band of antiferromagnetic  $2k_F$  charge density wave (CDW) structure. The CDWs also exhibit corrugation, and antiphase modulation, at  $a/2$  with respect to adjacent stacks. This is consistent with appreciable interstack Coulomb interactions and contributions from the magnetic  $4k_F$  structure, which based on the tight-binding approximation is equivalent to the canonical description  $(\text{TCNQ})_2^+(\text{TCNQ})_2^-$ . The STM data are in agreement with magnetic susceptibility and EPR studies, which indicate significant contribution of the  $4k_F$  state to the electronic structure of 1. The STM therefore provides characterization of the local electronic structure that is manifested in the bulk electronic properties of 1.

### Introduction

Crystalline solids based on molecular components exhibit numerous electronic phenomena, including electrical conductivity, superconductivity, nonlinear optical behavior, and ferromagnetism.<sup>1</sup> The most extensively examined molecular crystals have been the low-dimensional conductors and semiconductors, which generally exhibit anisotropic conductivity along axes containing stacks of open-shell charge-transfer molecules that are responsible for the formation of extended band structure. Most notable among low-dimensional molecular crystals are the organic superconductors<sup>2</sup> and, more recently, ferromagnetic materials based on metallocene salts of polycyanonions.<sup>3</sup> The observation of conductivity and magnetism in ex-

tended solids, particularly numerous charge-transfer salts of tetracyanoquinodimethane (TCNQ),<sup>4</sup> suggests a sig-

(1) (a) Lehn, J.-M. *Angew. Chem., Int. Ed. Engl.* 1988, 27, 89. (b) *Molecular Electronic Devices*; Carter, F. L., Ed.; Marcel Dekker, New York, 1982. (c) *Extended Linear Chain Compounds*; Miller, J. S., Ed.; Plenum: New York, 1982-1983; Vols. 1-3. (d) Desiraju, G. *Crystal Engineering*; Elsevier: New York, 1989. (e) Miller, J. S.; Epstein, A. J.; Reiff, W. M. *Science*, 1988, 240, 40.

(2) (a) Williams, J. M.; Carneiro, K. *Adv. Inorg. Chem. Radiochem.* 1985, 29, 249. (b) Inokuchi, H. *Angew. Chem., Int. Ed. Engl.* 1988, 27, 1747-1751. (c) Emge, T. J.; Leung, P. C. W.; Beno, M. A.; Wang, H. H.; Firestone, M. A.; Webb, K. S.; Carlson, K. D.; Williams, J. M.; Venturini, E. L.; Azevedo, L. J.; Schirber, J. E. *Mol. Cryst. Liq. Cryst.* 1986, 132, 363. (d) Montgomery, L. K.; Geiser, U.; Wang, H. H.; Beno, M. A.; Schultz, A. J.; Kini, A. M.; Carlson, K. D.; Williams, J. M.; Whitworth, J. R. *Synth. Met.* 1988, 27, A195.

(3) (a) Miller, J. S.; Epstein, A. J.; Reiff, W. M. *Acc. Chem. Res.* 1988, 21, 114. (b) Miller, J. S.; Epstein, A. J.; Reiff, W. M. *Science* 1988, 240, 40.

\* To whom correspondence should be addressed.